Exploring the influence of electron beam crosslinking in SEBS/TPU and SEBS-g-MA/TPU thermoplastic elastomer blends

Anagha, M. G.; Chatterjee, Tuhin; Picchioni, Francesco; Naskar, Kinsuk

Published in:
Journal of Applied Polymer Science

DOI:
10.1002/app.51721

Publication date:
2022

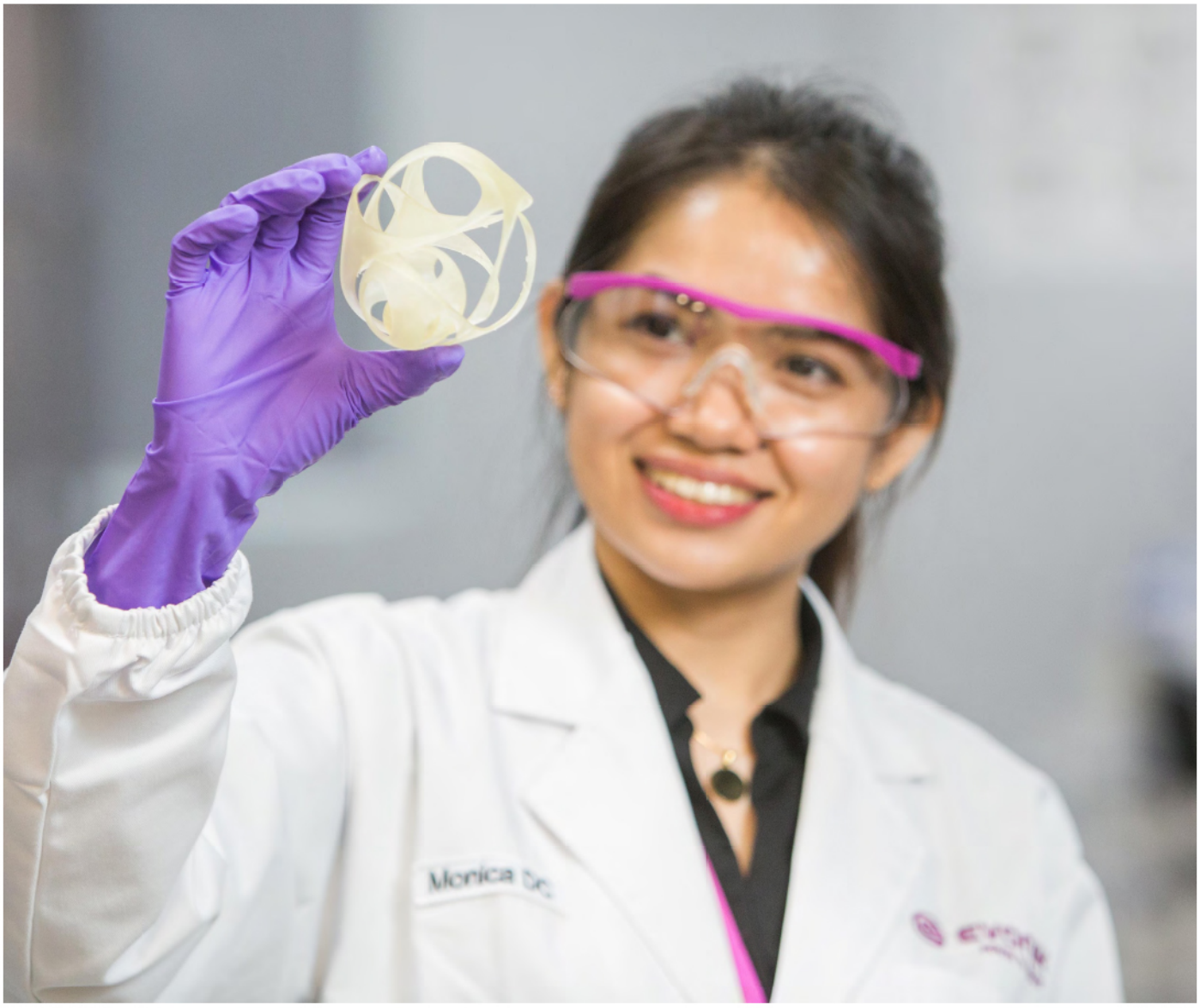

Pushing the boundaries of chemistry? It takes #HumanChemistry

Make your curiosity and talent as a chemist matter to the world with a specialty chemicals leader. Together, we combine cutting-edge science with engineering expertise to create solutions that answer real-world problems. Find out how our approach to technology creates more opportunities for growth, and see what chemistry can do for you at:

evonik.com/career

EVONIK
Leading Beyond Chemistry

Received: 9 June 2021 | Revised: 15 September 2021 | Accepted: 15 September 2021

DOI: 10.1002/app.51721

ARTICLE

Applied Polymer SCIENCE WILEY

Exploring the influence of electron beam crosslinking in SEBS/TPU and SEBS-g-MA/TPU thermoplastic elastomer blends

M. G. Anagha[1] | Tuhin Chatterjee[2] | Francesco Picchioni[2] | Kinsuk Naskar[1]

[1]Rubber Technology Centre, Indian Institute of Technology, Kharagpur, West Bengal, India

[2]Department of Chemical Engineering, University of Groningen, Groningen, Netherlands

Correspondence
Kinsuk Naskar, Rubber Technology Centre, Indian Institute of Technology, Kharagpur, West Bengal, India.
Email: knaskar@rtc.iitkgp.ac.in

Abstract

The effects of electron beam (EB) radiation in thermoplastic elastomers based on SEBS/TPU and SEBS-g-MA/TPU are evaluated. 60/40 blend of both the systems were subjected to EB using an ILU type industrial accelerator. Radiation dose was varied from 0 to 100 kGy, and the sol–gel content evaluation along with detailed analysis of mechanical, thermal, rheological, and morphological implications was conducted. The interplay between crosslinking and chain scission was quantified using the Charlesby-Pinner equation. Both the blends showed the presence of a three-dimensional cross-linked network in them after the irradiation. The tensile strength of SEBS/TPU was found to deteriorate with an increase in radiation dose, but an opposite trend was observed in SEBS-g-MA/TPU. Improvement in interfacial adhesion between SEBS-g-MA and TPU was confirmed. The morphological analysis through atomic force microscopy and scanning electron microscopy clearly showed the appearance of rough ridges and pits due to irradiation along with the cross-linked networks. From differential scanning calorimetry analysis, the changes in glass transitions and melting endotherm were assessed. Thermogravimetric analysis results indicated an improvement in the thermal stability of the blends. The storage modulus and complex viscosity of the samples enhanced as perceived from the rheological measurements. X-ray diffraction patterns of the blends also showed considerable variation after irradiation.

KEYWORDS

irradiation, morphology, mechanical properties, rheology

1 | INTRODUCTION

The influence of high-energy radiation on materials was a keen area of interest from the early 19th century. It was at the end of the 1930s that their effect in long chain polymers emerged as an essential field of research. Although there were many limitations concerned with the availability of energy sources, in the preceding years, sufficient sources became accessible. It led to an increased interest in radiation research on materials and the growth of the polymer industry.[1] Electron beam (EB) irradiation is one of the high-energy solid-state processes and is proven to be effective for various chemical changes in multiple polymers. Electrons fall into the high energy and short wavelength region in the electromagnetic spectrum with a wavelength range of 10^{-4}–10^{-2} nm.[2,3] The energy transferred from an EB is profoundly higher than the energy needed to break chemical bonds

in polymers.[3,4] For instance, the binding energy of a C-H bond is approximately 4.8 electron-volt (eV), while the energy of an EB is in the range of mega electron-volt (MeV). Besides, the method is eco-friendly, which makes it an imperative part of the green drive initiative.

These ionizing radiations, when interacting with polymers, knock off electrons and produce free radicals, which induce chemical reactions in them. Polymers, when subjected to radiation, can undergo three kinds of reactions; crosslinking, chain scission, and grafting.[3] The processes, crosslinking and chain scission tend to compete always and their balance depends on structural and experimental factors. The mechanism of crosslinking due to EB radiation is dependent on the nature of the polymers involved. EB irradiation is often used to improve interfacial adhesion in polymer blends via interfacial crosslinking. It has been reported that this is achieved by either physical linkages or by covalent bonds. In a polymer blend, the lifetime of the free radicals generated depends strongly on the structure and crystallinity of the phase in which the localization occurs.[5]

Thermoplastic elastomers (TPEs) constitute an important class of polymers with characteristic properties similar to that of elastomers at room ambient temperatures and can be processed like thermoplastics at higher temperatures.[6,7] EB modification on TPEs is comparatively a new technique to produce novel materials.[8–11] There are reported studies in which the elastomeric phase in a polyolefin/TPE blend is radiation crosslinked to improve the impact strength of the olefinic phase.[12,13] In the current study, TPEs based on styrene-ethylene-butylene-styrene (SEBS)/thermoplastic polyurethane (TPU) and maleated styrene-ethylene-butylene-styrene (SEBS-g-MA)/TPU are subjected to EB radiation, and the effects are investigated in detail. Although there are a few studies that explore these blend systems,[14,15] no study has been reported discussing the effect of EB exposure on them. Styrenic block copolymers and TPUs are the highly consumed polymers in the global TPE market. SEBS is widely used in applications like medical, construction, automotive, and consumer goods. SEBS-g-MA, on the other hand, is usually used as a compatibilizer for immiscible polymer blends.[16–18] TPU is a unique class of TPEs with outstanding elastomeric and mechanical properties along with solvent and chemical resistance.[19–21]

TPUs are found to be radiation resistant depending on their molecular structure, and a few studies have been reported regarding their EB modification. The effect of irradiation on the physical properties and chemical structure of aliphatic polyurethanes was explored by Adem et al.[22] It was concluded that both hard and soft segments are affected by radiation, but mechanical properties deteriorated since the crosslinking took place in the amorphous region. Murray et al. used a medical grade polyurethane to investigate the effect of radiation and found that a high degree of crosslinking takes place at high radiation doses, and the occurrence of phase separation was also reported.[23] They also reported notable changes in the morphology of the polymer. A few other papers have been published which deal with the radiation effects on TPU.[24,25] EB modification of blends of TPU with other polymers has also been explored and reported.[10,26]

Few papers are published which discuss the effect of the EB on SEBS blended with other polymers. As mentioned earlier, blends of olefinic polymers with SEBS block copolymers have been radiation modified to enhance the toughness of the former. Other studies include blends of low-density polyethylene (LDPE)/SEBS/SEBS-g-MA in which the incorporation of styrenic block copolymer improved the radiation induced properties of LDPE.[27] Although there are papers concerning the effect of the EB on polymer blends compatibilized with SEBS-g-MA or SEBS, there are very limited studies on the impact of EB radiation exclusively in SEBS or SEBS-g-MA.

The current work demonstrates in detail the influence of the EB in a 60/40 blend of SEBS/TPU as well as SEBS-g-MA/TPU. From this study, we aim to scrutinize the possibility of EB curing for improving the performance properties of the blends. These blends have been selected from previous studies conducted and published.[28,29] The exceptional characteristics of these three TPEs make them an excellent choice for the automotive industry. Their inherent characteristics, such as ease of processability, no requirement of additives, recyclability and so forth, makes them industrially attractive and possible alternatives to existing rubber parts. EB curing can be a fruitful way of crosslinking these polymers without having to add a third ingredient. Here, we have focused on the meticulous characterization of the blends in order to quantitatively assess the influence of EB radiation.

2 | EXPERIMENTAL

2.1 | Materials used

Styrene-ethylene-butylene-styrene used was Kraton G1633 E (Kraton, Belgium), a newly developed grade having ultra-high molecular weight. It is a clear linear triblock copolymer with a density of 0.91 g/cm^3 and 29.5% bound styrene content. Kraton FG 1901 G (Kraton, Belgium) was the maleic anhydride grafted SEBS used. It is also a clear linear triblock copolymer with a bound styrene content of 30%. TPU Desmopan, 385 L with a density of 1.2 g/cm3, was obtained from Bayer Chemicals, India. It is composed of 4,4'-diphenylmethane diisocyanate with polyester soft segments.

2.2 | Preparation of blends and EB irradiation

A Haake Rheomix OS (Germany) 600 was used to mix and prepare the TPE blends. It is an internal mixer having a chamber volume of 85 cm^3. The 60/40 blends of both SEBS/TPU and SEBS-g-MA/TPU were mixed at a temperature of 190°C and the mixing time was 10 minutes. At first, TPU was added and melt mixed for 2 min. Then SEBS/SEBS-g-MA (according to the formulation) was added and mixed for the next 6–8 min. The mixes were sheeted out while hot in an open mill set at 2 mm nip gap. The sheets were then stored at 23 ± 2°C and relative humidity of 50 ± 5% for 24 h. The sheets were compression molded for 4 min between teflon sheets at 200°C in an electrically heated hydraulic press (Moore Hydraulic Press, England). To preserve the total dimensional stability, the sheets were cooled under pressure.

EB irradiation of the molded sheets was carried out at Bhaba Atomic Research Centre (Mumbai, India). Irradiation was done in the air at room temperature with an ILU-6 electron-beam accelerator. Figure 1 illustrates the accelerating system of an ILU-6 accelerator. It is the base model among the ILU electron accelerator family and is suitable for creating an irradiation zone for applications involving polymers.[30]

Primarily, it accommodates a vacuum tank in which a toroidal resonator is installed. There are electrodes attached on both the up and bottom halves of the resonator. The cathode unit, together with the grid and the electrode in the top half, constitutes an electron gun. Whereas the accelerating system is formed by the bottom electrode and the injector. In the resonator's bottom half, a magnetic lens is installed, which forms an EB. An RF generator is inside the vacuum tank and connected to the resonator using a coupling loop.

For the irradiation of the samples, the radiation doses were varied from 10, 25, 50, and 100 kGy. The acceleration energy was 5.0 MeV, and the beam current was 17 mA. Different blends before and after irradiation are designated in Table 1 given below.

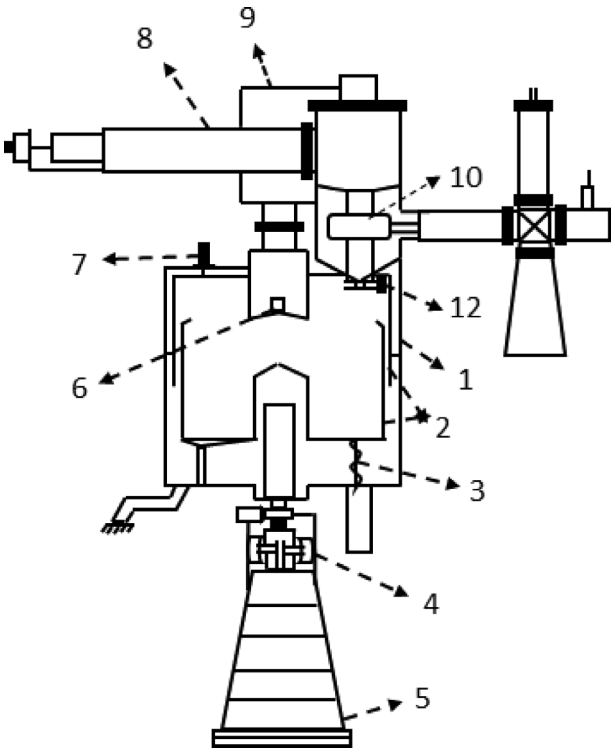

FIGURE 1 Important parts of an ILU-6 electron accelerator. (1) Vacuum tank, (2) Two part radio frequency (RF) cavity, (3) Voltage input, (4) High-vacuum pump, (5) Scanning horn, (6) Electron injector, (7) Measuring loop, (8) Cathode circuit tuning line, (9) High-vacuum pump, (10) RF generator and (11) Coupling loop

TABLE 1 Sample designation as a function of radiation dose

Sample	EB radiation dose (kGy)
$S_{60}T_{40}$–0 kGy	0
$S_{60}T_{40}$–10 kGy	10
$S_{60}T_{40}$–25 kGy	25
$S_{60}T_{40}$–50 kGy	50
$S_{60}T_{40}$–100 kGy	100
$M_{60}T_{40}$–0 kGy	0
$M_{60}T_{40}$–10 kGy	10
$M_{60}T_{40}$–25 kGy	25
$M_{60}T_{40}$–50 kGy	50
$M_{60}T_{40}$–100 kGy	100

Note: S = SEBS, M = SEBS-g-MA, T = TPU. $S_{60}T_{40}$ = 60/40 blend of SEBS/TPU, $M_{60}T_{40}$ = 60/40 blend of SEBS-g-MA/TPU.

2.3 | Characterization techniques

2.3.1 | Tensile properties

Tensile properties of the blends before and after EB irradiation were determined in a universal testing machine Hounsfield H25KS (UK) with a load cell of 10 kN, as per ASTM D 412. During the testing, crosshead speed was 200 mm/min, and the standard test temperature was 23 ± 2°C, and relative humidity of 50 ± 5% was maintained. Dumbbell specimens with 25 mm gauge length and 4 mm width were cut out from the molded sheets for the test. Each specimen was placed symmetrically in the grips of the UTM to uniformly distribute tension over the cross-section. For accurate results, four specimens from each sample were tested.

2.3.2 | Hardness

Workzone digital Shore A and D durometers were used to estimate the change in hardness of unirradiated as well as irradiated blends. The indentor of the durometer was placed parallel to the surface and pressed into the pile of specimens having a thickness of 6 mm. A total of five tests were done in order to attain a statistical measurement. All the readings were taken in 1 s.

2.3.3 | Sol and gel content analysis

Circular specimens (~1.3 mm dia) of approximately 0.25 g were accurately weighed and immersed in toluene for 3 days (72 h) at room temperature. After the immersion period, the samples were taken out and wiped with tissue to remove excess solvent and weighed to obtain the swollen weight. Then they were dried in an air oven to constant weight. Sol and gel content of different samples were calculated using Equation (1):

$$g = \frac{w_2}{w_1} \times 100 \quad (1)$$

where g is the gel fraction, w_2 is the weight of dried network polymer, and w_1 is the initial weight of the polymer, and *1-g* gives the sol fraction.

2.3.4 | Scanning electron microscopy

A Field Emission Scanning Electron 348 Microscope, Merlin (Germany), was used to examine the microstructure of the blends exposed to EB radiation. All the samples were cryofractured in liquid nitrogen and dried prior to observation. All the samples were sputtered with gold to impart conductivity. The magnification was 5kX, and the accelerating voltage was 5 kV, and an in-lens detector was used.

2.3.5 | Atomic force microscopy

To quantitatively probe the morphology of the blends in concern, ACAFM (Agilent 5500 Scanning Probe Microscope, USA) was used. For the analysis of soft polymers like TPEs tapping mode (intermittent contact mode), atomic force microscopy is used.[18,31] The AFM tip was made of silicon nitride, with a radius of curvature 10 nm. The cantilever frequency was 150 kHz, and the force constant was 42 N/m. Samples were carefully cut from the 2 mm × 2 mm molded sheets.

2.3.6 | Rheological measurements

A TA Discovery HR-2 hybrid rheometer (USA) with a gap size of 1000 micrometers was used to carry out rheological measurements in parallel plate geometry. The rheometer is equipped with 8 mm diameter parallel plates made of stainless steel. The viscoelastic properties of the samples were recorded as a function of frequency. The temperature of testing was 200°C, and the frequency range was from 0.05 to 100 rad/s.

2.3.7 | Differential scanning calorimetry

The variation in glass transition temperatures, as well as melting behavior of the blends as a result of EB irradiation, were investigated using a Netzsch differential scanning calorimetry (DSC) (Germany). All the samples were heated from −80 to 200°C with a heating rate of 10°C/min and then cooled to −80°C and again heated to 200°C. To disregard the thermal history of the samples, the readings from second heating scans were analyzed.[32–35]

2.3.8 | Thermogravimetric analysis

The thermal stability of different blend systems was accessed using a Perkin Elmer thermogravimetric analysis (TGA) 4000 (USA). The samples were heated from 30°C to 700°C in a nitrogen atmosphere. The heating rate was 10°C/min. The tests were repeated to ensure the accuracy of the results.

2.3.9 | X-ray diffraction

X-ray diffraction (XRD) analysis of the samples was carried out in the wide-angle range using a Bruker diffractometer (UK). The wavelength of the X-ray was 1.54 Å (Cu Kα radiation), and the angular range (2θ) was varied between 5° and 50°.

3 | RESULTS AND DISCUSSION

3.1 | Physicomechanical properties

Figure 2a, b depicts the stress–strain behavior of non-irradiated and EB irradiated (at different radiation dosage) various SEBS/TPU blends and SEBS-g-MA/TPU blends, respectively.

When a polymeric material is exposed to radiation such as γ-ray, x-ray or EB crosslinking (x) and chain

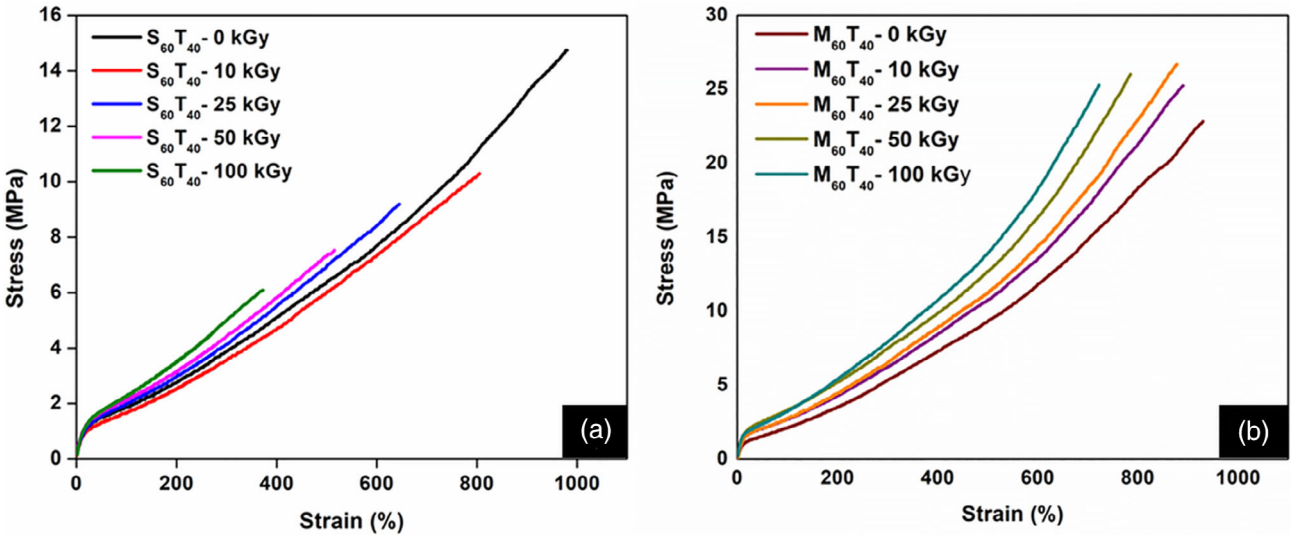

FIGURE 2 Stress–strain curves of (a) $S_{60}T_{40}$ (b) $M_{60}T_{40}$ blends before and after irradiation [Color figure can be viewed at wileyonlinelibrary.com]

scission (s) process always co-exist. Generally, crosslinking enhances the mechanical properties and thermal stability of the polymer while reducing the melt flow rate and increases the viscosity at the same time. On the other hand, chain scission deteriorates the mechanical properties and thermal resistance and increases the melt flow rate. Generally, radiation chemists use the term G value, which is defined as the chemical yield of radiation in the number of molecules reacted per 100 eV of absorbed energy. Therefore, whenever G(x) is larger than G(s), that is, G(s):G(x) ratio < 1, the overall predominating result is crosslinking, and whenever G(s) is larger than G(x), that is, G(s):G(x) ratio > 1, the predominating result is degradation or chain scission of the polymer chain.

Considering Figure 2a, it can be noticed that after the EB treatment, there is deterioration in the stress–strain properties in terms of the tensile strength (TS) and elongation at break (%EB) for the SEBS-TPU blend system. Compared to nonirradiated blend, the TS and %EB of the EB irradiated blends is much lower. This declination could be attributed to the following reasons; As noted from various studies, TPU is radiation-resistant to an extent. The used dosage of 10–100 kGy may not be sufficient enough to bring about crosslink networks in the polymer. So, in SEBS/TPU blends, SEBS being the amorphous phase, the chances of chain crosslinking are higher. Also, owing to the incompatibility between SEBS and TPU, the contribution of interfacial crosslinking between SEBS and TPU to tensile properties is less. In addition, the breakage of the crystalline structure of the polymer backbone upon the treatment of the EB is also a possibility. The TPU phase in the blend is semicrystalline due to aggregates of hard segments in them.[7] The effects of the EB radiation on crystallinity is discussed elsewhere in this paper.

From Figure 2b, it can be observed that there is a fair improvement in the stress–strain properties of the SEBS-g-MA/TPU blend system after the EB treatment. Hence, it can be inferred there is indeed interfacial crosslinking and formation of three-dimensional crosslinked networks in the blends. Also, the compatibility between SEBS-g-MA and TPU is improved as an outcome of the irradiation process. The values of TS, elongation at break (%EB), modulus at different elongations, modulus of toughness, and Shore hardness of both the blend system before and after EB irradiation are tabulated in Table 2.

Following the table, it can be seen that for the nonirradiated $S_{60}T_{40}$ blend, the TS and %EB are 14.9 MPa and 971%, respectively. With the treatment of the EB, both TS and %EB gradually come down to lower values for the irradiated $S_{60}T_{40}$ blend. For example, the TS and %EB of $S_{60}T_{40}$–10 kGy blend system is 10.6 MPa and 782%, respectively, and it goes down further to 6.1 MPa and 368%, respectively, for the $S_{60}T_{40}$–100 kGy blend system. It is also known that the area under the stress–strain curve relates to the toughness of the material. From the table, it can also be noticed that the modulus of toughness decreases proportionally for $S_{60}T_{40}$ blends with the increase in radiation dose. However, the improvement in modulus value and hardness value (shore A and shore D) indicates the presence of crosslinked network structures. Considering the table, it can be viewed that the modulus value at 300% elongation increases from 3.8 MPa for the nonirradiated blend to 5.1 MPa for the $S_{60}T_{40}$–100 kGy

TABLE 2 Physicomechanical properties of nonirradiated and irradiated blends

Sample	Tensile strength (TS) (MPa)	Elongation at break %EB (%)	Modulus at		Modulus of toughness ($M.J./m^3$)	Hardness	
			100% elongation (MPa)	300% elongation (MPa)		Shore A	Shore D
$S_{60}T_{40}$–0 kGy	14.9 ± 0.2	971 ± 7	1.9 ± 0.0	3.8 ± 0.1	6.6 ± 0.4	71.0 ± 0.5	22.0 ± 0.4
$S_{60}T_{40}$–10 kGy	10.6 ± 0.3	782 ± 14	1.7 ± 0.1	3.5 ± 0.1	4.1 ± 0.5	74.0 ± 0.1	24.0 ± 0.1
$S_{60}T_{40}$–25 kGy	9.3 ± 0.4	661 ± 16	1.8 ± 0.0	3.9 ± 0.2	3.0 ± 0.6	78.0 ± 0.5	25.0 ± 0.2
$S_{60}T_{40}$–50 kGy	7.3 ± 0.4	512 ± 20	2.1 ± 0.1	4.2 ± 0.1	2.1 ± 0.3	78.8 ± 0.8	24.5 ± 0.5
$S_{60}T_{40}$–100 kGy	6.1 ± 0.4	368 ± 21	2.2 ± 0.2	5.1 ± 0.1	1.3 ± 0.5	80.6 ± 0.2	24.5 ± 0.3
$M_{60}T_{40}$–0 kGy	23.1 ± 0.4	940 ± 7	2.2 ± 0.2	5.3 ± 0.3	9.0 ± 0.5	80.5 ± 0.1	28.5 ± 0.5
$M_{60}T_{40}$–10 kGy	25.4 ± 0.8	871 ± 24	2.7 ± 0.3	6.2 ± 0.4	9.5 ± 0.4	81.1 ± 0.4	29.0 ± 0.4
$M_{60}T_{40}$–25 kGy	27.3 ± 0.5	850 ± 21	2.8 ± 0.2	6.7 ± 0.2	9.8 ± 0.7	81.8 ± 0.7	28.5 ± 0.2
$M_{60}T_{40}$–50 kGy	26.8 ± 0.8	795 ± 25	3.3 ± 0.1	7.4 ± 0.3	8.6 ± 0.3	82.5 ± 0.8	28.5 ± 0.6
$M_{60}T_{40}$–100 kGy	25.4 ± 0.4	720 ± 10	3.4 ± 0.1	8.2 ± 0.1	7.7 ± 0.5	83.6 ± 0.6	29.5 ± 0.4

blend system. It also implies the formation of the crosslinked network structure in the polymer backbone in the presence of EB on the other side. It should be noted here that with TS and %EB, the modulus value of the $S_{60}T_{40}$–10 kGy blend is also lower than the virgin $S_{60}T_{40}$ blend. From this scenario, it can be argued that maybe the polymer chain scission phenomenon is the most occurring one in the case of $S_{60}T_{40}$–10 kGy blend. This similar trend has been observed in the rheology study, the thermogravimetric study also. Simultaneously, the shore A and shore D hardness value also increases from 71 shore A for the nonirradiated blend to 80.6 shore A for the $S_{60}T_{40}$–100 kGy blend and 22 shore D to 24.5 shore D for the $S_{60}T_{40}$–100 kGy blend, respectively.

From the table, at the same time, it can be evidently seen that after the EB treatment, there is a sharp improvement in stress–strain properties for the m-SEBS/TPU blend system. Almost 18% improvement in TS occurred with 25 kGy of radiation dose. Subsequently, with high doses of EB, the strength diminishes marginally. But there is no significant deterioration of TS, which indicates the stability of the blends towards EB radiation. The %EB value drops down from 940% for the nonirradiated mSEBS-TPU to 720% for the $M_{60}T_{40}$–100 kGy blend system, which indicates the reduction in chain mobility of the polymer due to the formation of the crosslinked network structure. It should be noted here that the reduction in elongation at break and hence the toughness in this blend system is less pronounced than that witnessed in the SEBS/TPU system. Meanwhile, the modulus of the blends is found to improve significantly with radiation dose. There is a 54% increase in modulus at 100% elongation when compared to the nonirradiated blend. Similarly, modulus at 300% elongation boosted to 55% with exposure to 100 kGy. This increment is modulus value indicates the formation of the crosslinked network structure in the presence of the EB. Thus, two possibilities can be inferred from here. The EB induced curing may have boosted up the interfacial interactions between SEBS-g-MA and TPU. Also, the presence of maleic anhydride groups in the former might have favored the crosslinking upon radiation exposure. Considering the results, it can be indicated that in SEBS-g-MA/TPU blends, the optimum TS is achieved at a radiation dose of 25 kGy. At even higher doses, the property deteriorates.

3.2 | Sol and gel fraction analysis

In the previous section, we discussed the phenomenon of crosslinking and chain scission in the samples after the EB exposure and their effect on the mechanical properties. This leads us to the mechanism of chain crosslinking and chain scission as a result of EB radiation. Polymers, when subjected to high-energy radiation sources, tend to dimerize by linking of molecules. This is initiated by the formation of radicals, which is discussed in the introduction before. As a consequence of dimerization, a three-dimensional network is formed similar to that in a vulcanized rubber. The radiation dose at which the gelation starts to occur is termed as the gelling dose, and the point at which it begins first is the gel point. Chain scission, similar to chain crosslinking, occurs simultaneously and results in the splitting up of a single polymer chain into fragments.

The radiation processing of polymer blends is different from that of a single polymer. The phase in which crosslinking or chain scission occurs depends upon the

structure of the individual polymer. From earlier studies, it has been found that the chance of crosslinking is more favored in copolymers with high branching density during EB radiation treatment.[36,37] Also, there is a probability of compatibilization of the polymers as a result of the interfacial cross-linking, as suggested before. The relation of radiation dose with the degree of crosslinking and the degree of degradation is perceivable from the sol–gel analysis.[1] The sol fraction necessarily contains the polymer molecules which does not possess any crosslinked networks while the gel fraction is left with the crosslinked polymer molecules.

The gel fraction of the polymer samples prior to and after radiation were calculated, and their dependence on the radiation dose is given in Figure 3.

In the unirradiated parent blends, the measured gel fraction can be attributed to the presence of physical crosslinks.[38] In $S_{60}T_{40}$ blend at 10 kGy, the gel fraction drops from 40% to 36%, indicating the possibility of chain scission at that particular dosage. At higher dosages, however, the gel fraction tends to increase, indicating the probability of crosslinking between the polymer chains. The value of the gel fraction rises to 74%, 85%, and 91% at EB doses of 25, 50, and 100 kGy, respectively. While in $M_{60}T_{40}$ system, the gel fraction increases gradually with the radiation dose. It reaches a maximum of 84% at 100 kGy. At higher radiation levels, the number of free radical formed increases, and there is a possibility of the formation of a higher fraction of crosslinked networks by the radicals recombining. However, at the same time, chances of chain scission also occur, keeping gel fraction at an optimum level.[39] Hence it can be inferred from the findings that crosslinking and chain scission take place simultaneously in both the systems.

The extent of crosslinking in the polymer systems under concern was quantified using the Charlesby-Pinner equation,[1,3,40–42] which is as follows:

$$s+\sqrt{s}=\frac{p_0}{q_0}+\frac{10}{q_0.u.D} \quad (2)$$

where s is the sol fraction, p_0/q_0 is the ratio of the probability of chain scission to that of crosslinking, u is the number average degree of polymerization, and D is the radiation dose in kGy. Figure 4 below depicts the Charlesby-Pinner plot with $s + \sqrt{s}$ versus the inverse of radiation dose.

The Charlesby-Pinner plot elucidates the extent of crosslinking and chain scission in the blend systems. As expected, the sol fraction s decreases with the radiation dose D in line with the gel fraction analysis done before. In a case where both crosslinking and chain scission occur during the radiation, the sol content s never becomes zero but depends upon the ratio of crosslinking to chain scission.[1] From the graph, it is noticeable that the crosslink networks are higher in $S_{60}T_{40}$ system than $M_{60}T_{40}$ system. However, the mechanical properties of the former system are inferior to that of the latter. It infers that in SEBS/TPU blend system, the crosslinking takes place in more individual phases rather than at the interfacial level. SEBS being less radiation-resistant than TPU, generates free radicals, resulting in cross-linked networks within the polymer. The quaternary carbon atoms in SEBS dissociates into

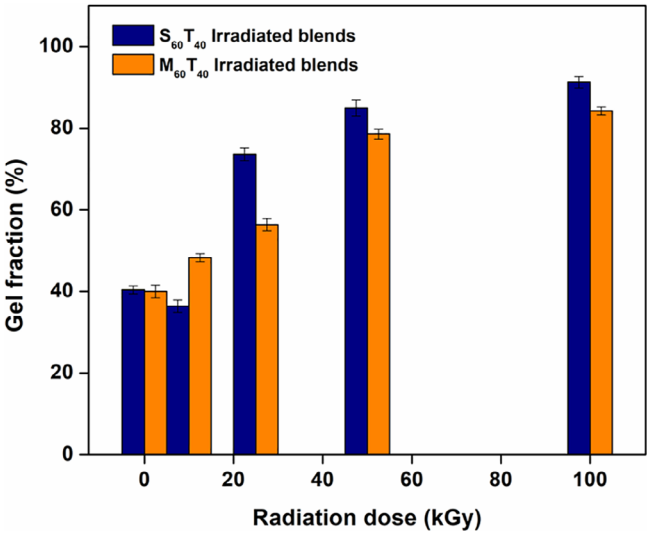

FIGURE 3 Gel fraction of $S_{60}T_{40}$ and $M_{60}T_{40}$ blends with respect to radiation dose [Color figure can be viewed at wileyonlinelibrary.com]

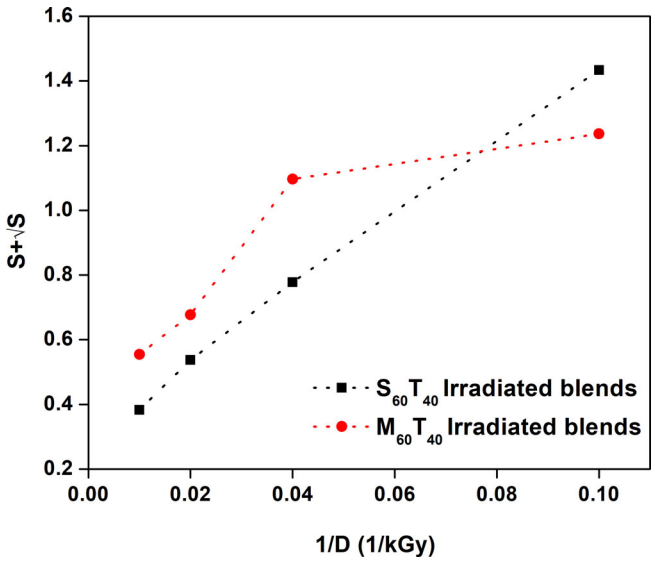

FIGURE 4 Charlesby-pinner plot [Color figure can be viewed at wileyonlinelibrary.com]

free radicals upon EB radiation exposure and initiate the chain crosslinking. In addition, it is known that at higher radiation doses, the polymer backbone degrades into smaller chains, which become individual crosslinked network clusters. These act as separate entities, and the forces holding together the clusters are sometimes not sufficient to withstand external forces like during tensile testing.[9,10] The deterioration of mechanical properties with an increase in radiation dose can be corroborated with this. In the case of SEBS-g-MA, the C═O bonds and the quaternary carbon atoms are the free radical generation sites that help in the instigation of crosslinking in the individual polymer phase and the interfacial crosslinking.[28] The higher compatibility and improved interfacial interaction between the blend components in SEBS-g-MA/TPU due to the radiation curing system also play a key role in achieving superior properties.[29]

3.3 | Scanning electron microscopy

The influence of EB radiation on the morphology of the blend systems under consideration was comprehended using scanning electron microscopy (SEM) as well. Understanding the microstructure of polymer blends is imperative since the physicomechanical properties of these are strongly dependent on the morphology. The SEM photo-micrographs of the fractured surface of the SEBS/TPU blend system after EB irradiation are presented below.

SEBS and TPU being thermodynamically immiscible exist in two-phase morphology.[18] This is clearly visible from Figure 5a–d and can be correlated to the inferior TS reported earlier. The interface, however, is not homogenized with an increased dose of EB radiation. Although, there are perceptible changes in the fracture surface at especially at higher radiation doses. These changes can be regarded as the results of surface oxidation associated with the EB exposure.

Figure 6a–d depicts the irradiated SEBS-g-MA/TPU 60/40 blend system. As expected from our previous studies[29] the blend components are mutually compatible with each other. The SEM images exhibit a uniform morphology of the concerned blends. The images of the two different images of both SEBS/TPU and SEBS-g-MA/TPU systems in juxtaposition evidently explains the extent of thermodynamic miscibility in the samples. The stabilized morphology of the latter is consistent as can be visualized from Figure 6a–d. In the following section, the changes in the morphology of the blends are comprehended and quantified.

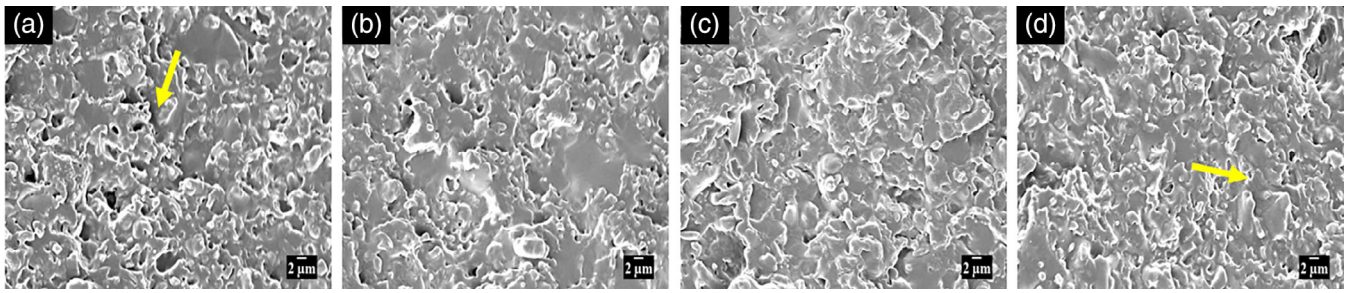

FIGURE 5 Scanning electron microscopy (SEM) photo-micrographs of (a) $S_{60}T_{40}$–10 kGy, (b) $S_{60}T_{40}$–25 kGy (c) $S_{60}T_{40}$–50 kGy (d) $S_{60}T_{40}$–100 kGy [Color figure can be viewed at wileyonlinelibrary.com]

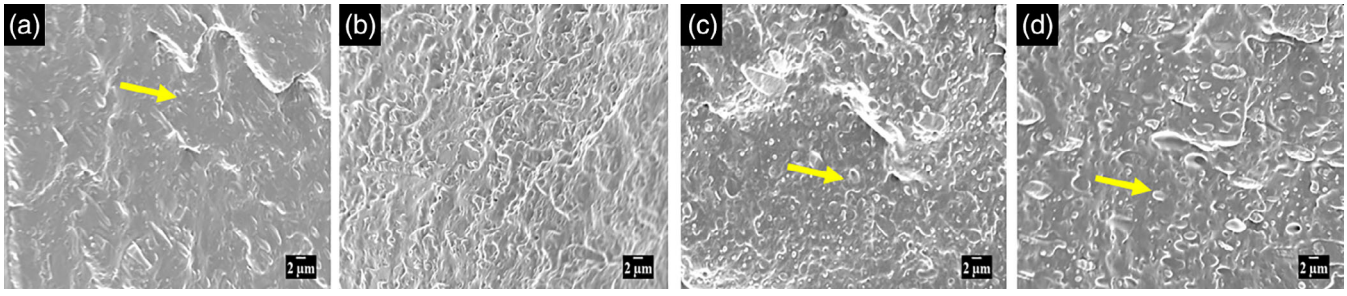

FIGURE 6 Scanning electron microscopy (SEM) photo-micrographs of (a) $M_{60}T_{40}$–10 kGy, (b) $M_{60}T_{40}$–25 kGy (c) $M_{60}T_{40}$–50 kGy (d) $M_{60}T_{40}$–100 kGy [Color figure can be viewed at wileyonlinelibrary.com]

3.4 | Atomic force microscopy

The surface morphology of the SEBS/TPU and SEBS-g-MA/TPU blends before and after EB irradiation is effectively deduced using the high-resolution Atomic Force Microscope. Figure 7a–h shows some selected phase and 3-D images of SEBS/TPU and SEBS-g-MA/TPU blends before and after irradiation. Every scan constitutes 10 μm × 10 μm lateral area. Figure 7a depicts the SEBS/TPU blend before irradiation with the EB, and (b), (c), and (d) are those of blends irradiated with 10, 50, and 100 kGy doses, respectively. From our previous studies[18,29] and as reported by various other researchers,[43,44] the dark regions in the AFM micrographs are considered as the soft phase and the brighter regions as hard phase. Accordingly, the brighter TPU domains are distributed along the darker SEBS matrix. The transition in surface morphology as the radiation dose increases is distinctively observable from Figure 7a–d. As the density of crosslinks rises in the blends, the brighter regions become dense. It is indicative of the crosslinked networks, which act as the hard phase. Figure 6 also encloses the 3-D height images of the blends, giving a three-dimensional view of the blend surface. They give a direct idea of the roughness of the blend surface up to a few micrometers. As can be seen from the figures, the roughness of the samples reduces as a result of irradiation.

Figure 7e–h depicts the AFM phase and 3-D height images of the SEBS-g-MA/TPU system subjected to EB irradiation. The parent blend $M_{60}T_{40}$–0 kGy being reactive in nature consists of a well-dispersed morphology in which TPU domains are uniformly distributed in the SEBS-g-MA matrix. This is well perceived from the 3-D height image given in Figure 7e with a comparatively smoother surface than the previous system. From the

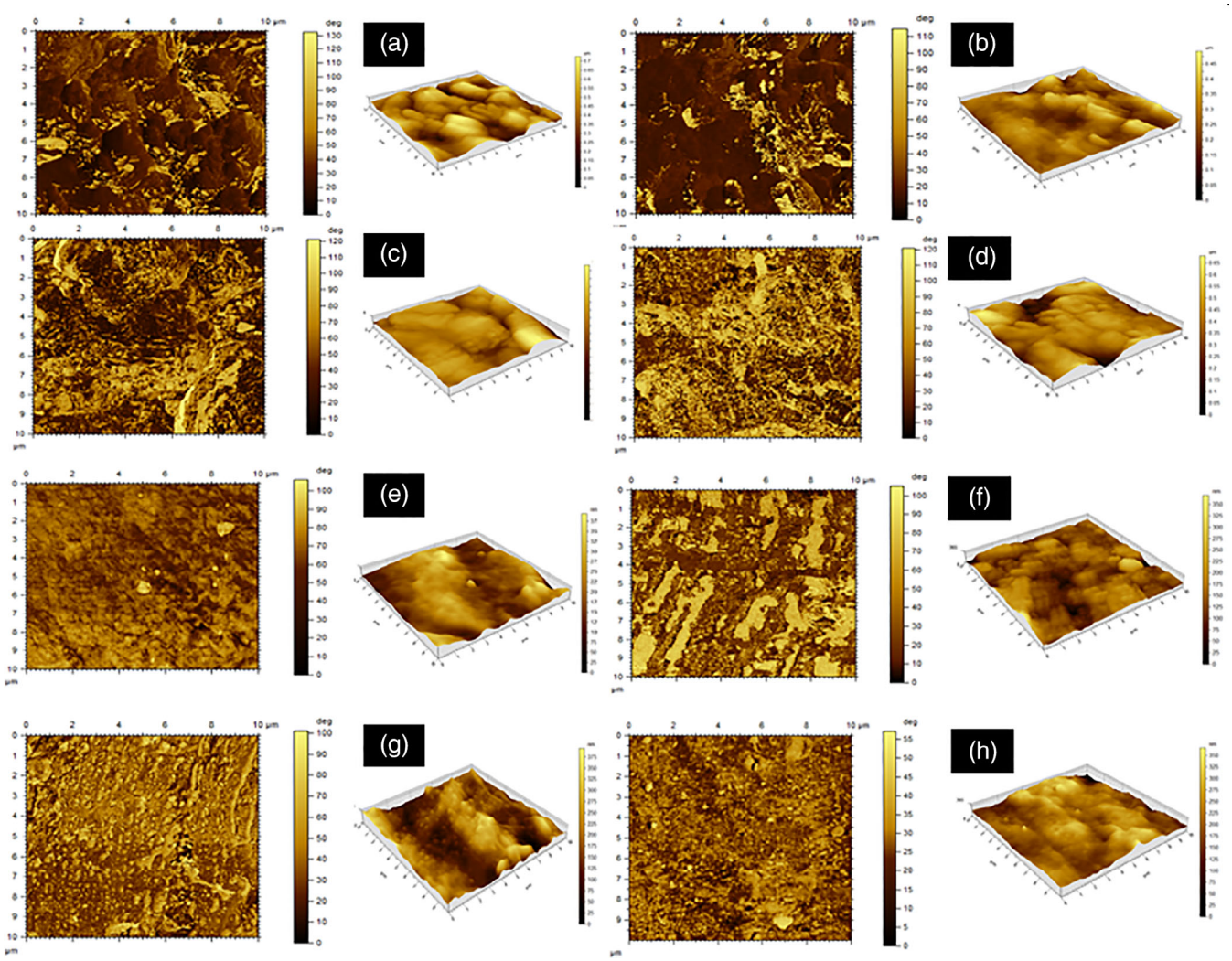

FIGURE 7 AFM phase and 3-D height images of (a) $S_{60}T_{40}$–0 kGy (b) $S_{60}T_{40}$–10 kGy (c) $S_{60}T_{40}$–50 kGy (d) $S_{60}T_{40}$–100 kGy (e) $M_{60}T_{40}$–0 kGy (f) $M_{60}T_{40}$–10 kGy (g) $M_{60}T_{40}$–50 kGy (h) $M_{60}T_{40}$–100 kGy [Color figure can be viewed at wileyonlinelibrary.com]

AFM phase images of irradiated blends given consecutively similar observations as above were obtained. With respect to the dose of EB irradiation, the concentration of the brighter region increases signifying the formation of cross-linked networks in the blends. At higher doses of radiation, both the systems show aggregates of cross-linked structures identifiable as the clusters of brighter regions in the phase images.

3.4.1 | Surface roughness parameters

A comparison of blend surfaces can be made with the use of roughness parameters. From the one- or two-dimensional surface topographical data, the surface roughness parameters are devised.[45] Among them, average surface roughness (R_a) and root mean square surface roughness (R_q) is of frequent use. They are given in Equation (3) and (4);

$$R_a = \frac{1}{n}\sum_{i=1}^{n}|z_i| \tag{3}$$

$$R_q = \left(\frac{1}{n}\sum_{i=1}^{n} z_i^2\right)^{\frac{1}{2}} \tag{4}$$

where n stands for the number of discrete profile variations, and z_i corresponds to the depth or height of the ith highest or lowest deviation.[29,31,45,46] These parameters do not give absolute values of roughness since they are dependent on the treatment of surface data as well as the AFM tip's curvature and size. During EB treatment, the material absorbs the energy associated with the electrons and heats up. It then evaporates and leads to sputtering thereby changing surface roughness.[47,48] Therefore, the evaluation of roughness parameters plays an imperative role in determining the effects of EB exposure in the polymer systems. The Table 3 below summarizes R_q and R_a values of the radiation treated blend systems.

The data reveal that the blend surface undergoes significant changes after EB irradiation. R_q and R_a values decrease after 10 kGy of radiation dose, indicating that the surface became smoother with 10 kGy dose owing to the sudden exposure of the polymer to EB. However, it is intriguing to

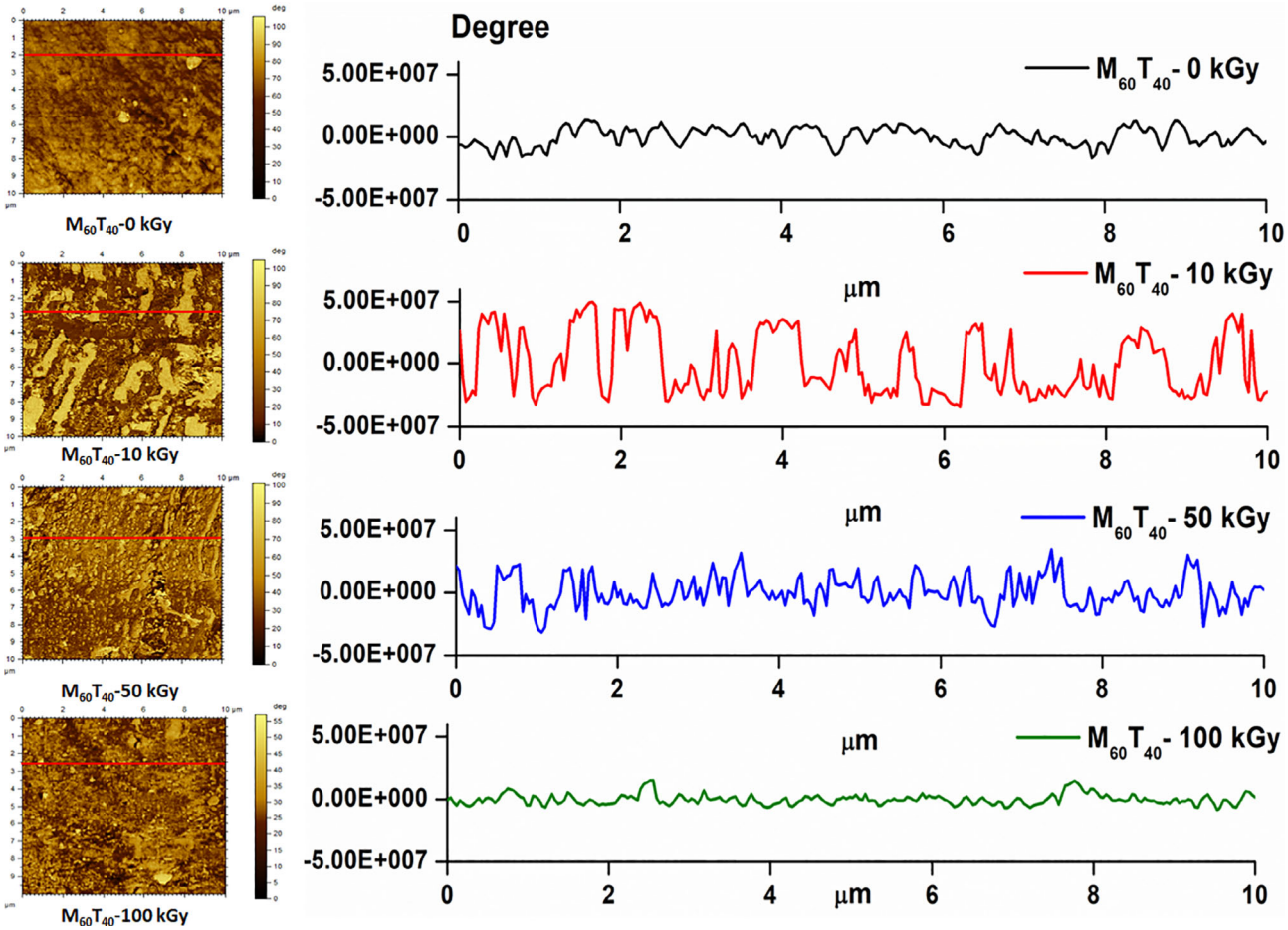

FIGURE 8 Line profiles of selected $M_{60}T_{40}$ blend before irradiation and after various radiation doses [Color figure can be viewed at wileyonlinelibrary.com]

note that as the radiation dose increases, the blend surface becomes rougher. Also, the number of yellow mounds is found to increase consistently with the radiation dose. It can be related to the change in crosslinking density as well as the events of chain scission and degradation.[49,50] In both the blend systems, the roughness parameters change more or less in a similar pattern. From the table, it can be noted that SEBS-g-MA/TPU blends have a smoother surface when compared to SEBS/TPU blends, owing to the better compatibility of the components. It can also be referred from the table that at 100 kGy the roughness values drop for both the blends. At higher doses, the surface protuberances come in close proximity to one another hence the surface area decreases. This results in the reduction in roughness values of the samples.[47]

3.4.2 | Profile analysis

A profile analysis of SEBS-g-MA/TPU blends was done to pursue the ramifications of the EB on the blend surface better. A line profile from AFM is a plot between vertical displacement and distance measured by scanning the specimen surface line by line. In Figure 8, the line profiles along with the phase images of $M_{60}T_{40}$ blend before and after radiation are given.

The change in the microstructure of the blend, when subjected to EB radiation, is well perceived from the images. As observed from the roughness parameters, EB exposure resulted in the rougher surface of the blends due to the introduction of a greater number of pits and valleys. The increase in the yellow mound count can also be correlated here. However, at 100 kGy, the displacement in the profiles can be seen to stabilize as a consequence of crosslinking and related homogenization in the blend agreeing with the data in Table 3.

TABLE 3 Roughness parameters of the blends from AFM

Sample	Root mean square surface roughness R_q (nm)	Average surface roughness R_a (nm)
$S_{60}T_{40}$–0 kGy	119.0 ± 3	90.0 ± 4
$S_{60}T_{40}$–10 kGy	69.0 ± 4	54.1 ± 3
$S_{60}T_{40}$–25 kGy	155.0 ± 5	122.0 ± 3
$S_{60}T_{40}$–50 kGy	220.0 ± 2	170.0 ± 2
$S_{60}T_{40}$–100 kGy	110.0 ± 5	80.0 ± 4
$M_{60}T_{40}$–0 kGy	65.4 ± 4	55.6 ± 3
$M_{60}T_{40}$–10 kGy	41.5 ± 4	31.5 ± 1
$M_{60}T_{40}$–25 kGy	72.0 ± 2	57.0 ± 3
$M_{60}T_{40}$–50 kGy	69.0 ± 3	56.5 ± 5
$M_{60}T_{40}$–100 kGy	55.7 ± 6	44.2 ± 1

3.5 | Parallel plate rheometer

Monitoring the shear rheology of the samples is an effective method to estimate the slightest differences in their structure. EB irradiation of SEBS/TPU and SEBS-g-MA/TPU blends resulted in various morphological and structural changes, as witnessed earlier. The rheology of polymer blends is highly influenced by crosslinking, chain branching, and chain scission of polymer chains. Changes in the microstructure of the blends can be deduced from the viscoelastic response to varying amplitudes of frequency.[51] Variations in storage modulus (G′) and complex viscosity (η*) with an increase in angular frequency (ω) were monitored. Figure 9 illustrates the storage modulus versus frequency of $S_{60}T_{40}$ and $M_{60}T_{40}$ blend systems before and after irradiation.

Figure 9(a), (b) are double logarithmic graphs of storage modulus and angular frequency. Storage modulus is indicative of the elastic nature of the material, and the plot explains the relative motion of the molecules. Also, G′ versus ω helps in better comprehending the flow behavior of the polymer blends.[18,52] Considering the first set of irradiated blends given in Figure 9a, it can be observed that initially, at lower frequencies, G′ increases slowly, and the increase is nominal at higher ranges. Blends with lower doses of irradiation depict more or less similar behavior like the unirradiated blend. With 10 kGy dose, the storage modulus of the SEBS/TPU blend falls below that of the parent blend. It can be inferred from here that in this blend, the phenomenon of chain scission predominates and hence results in the inferior properties. The introduction of the EB into the blend destroyed the crystalline structures, resulting in the deterioration of physicomechanical properties witnessed earlier. Hence it can be revalidated here that in $S_{60}T_{40}$ blends, chain scission favors at 10 kGy radiation dose. On the other hand, it is discernible from the plot that in highly irradiated blends, the storage modulus value ascends to as high as 100,000 Pa and more. It is achieved in systems with 50 kGy and 100 kGy radiation doses. It indicates the formation of three-dimensional polymer networks[51] hence improved elasticity of the blends at high doses of EB radiation. It is interesting to note that in the storage modulus of maleated SEBS/TPU blends, the effect of EB radiation is similar to that of SEBS/TPU blends witnessed above.

Logarithmic plots of angular frequency and complex viscosity of both the polymer systems are presented in Figure 10. Complex viscosity of the TPEs, irrespective of crosslinks, decreases with a rise in frequency, signifying the

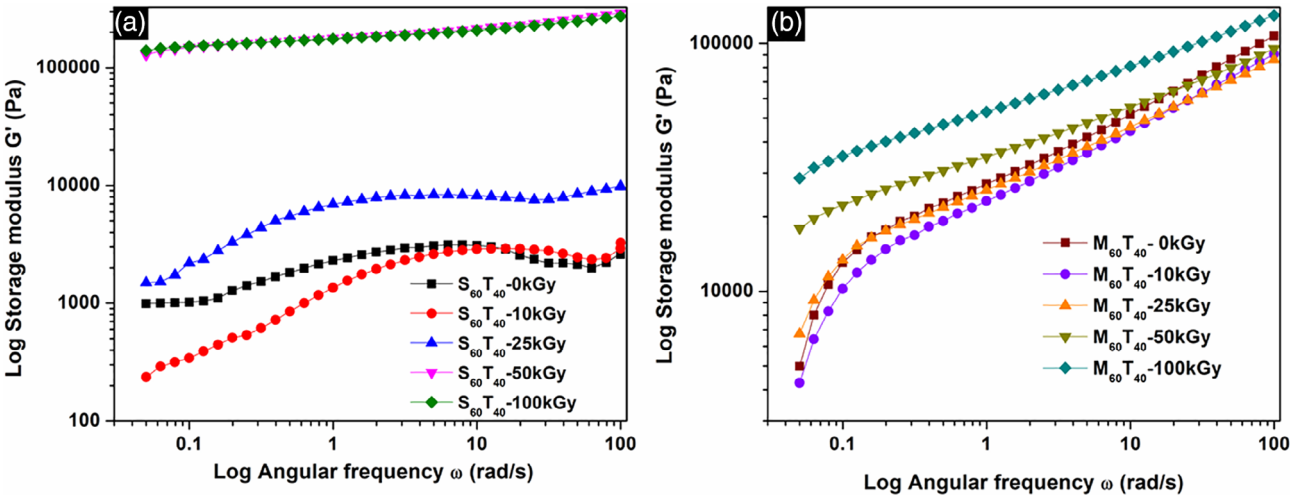

FIGURE 9 Storage modulus versus angular frequency of (a) $S_{60}T_{40}$ blends (b) $M_{60}T_{40}$ blends before and after irradiation [Color figure can be viewed at wileyonlinelibrary.com]

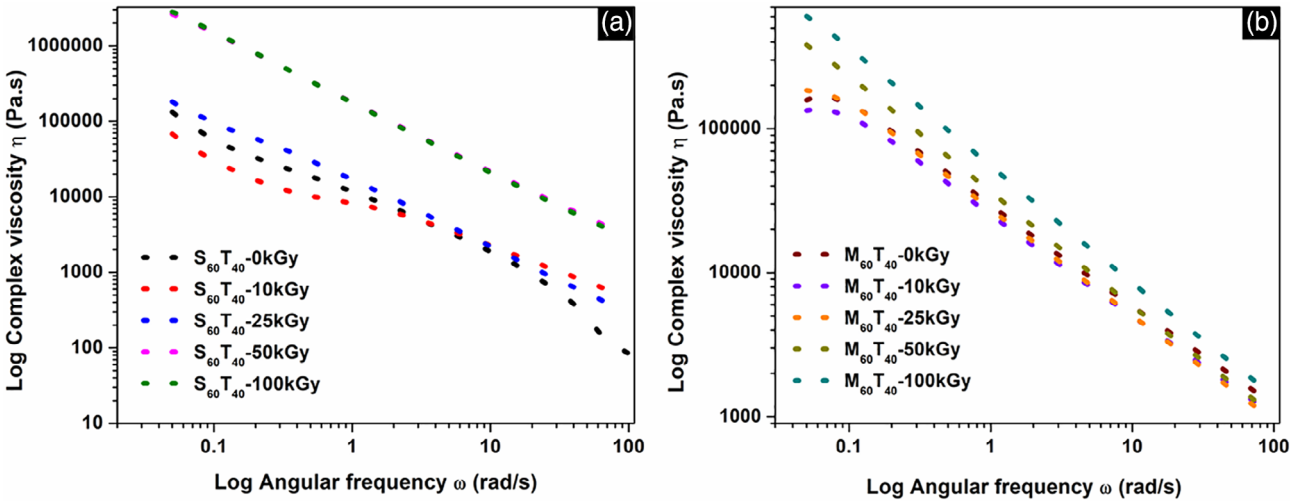

FIGURE 10 Complex viscosity versus angular frequency of (a) $S_{60}T_{40}$ blends (b) $M_{60}T_{40}$ blends. Values of complex viscosity, slope, and consistency index at an angular frequency of 0.05 rad/s are given in Table 4 [Color figure can be viewed at wileyonlinelibrary.com]

shear thinning behavior. Macromolecules, with their random orientation and entangled chains, when exposed to high shear environments, disentangle, and orient. This explains the pseudoplastic nature of the polymers.[18,26,53] The Power law can be suitably used to explain the complex viscosity curve at low frequencies, which is given in Equation (5);

$$\eta^* = k\omega^n \quad (5)$$

where η^* is the complex viscosity, ω is the angular frequency, k is the consistency index or viscosity coefficient index,[55] and n is the shear thinning exponent.

With the introduction of EB radiation in the samples, the complex viscosity showed a notable change in both the systems. The viscosity of the blends rose profoundly at higher radiation doses due to dimerization.[1] It has been understood from the findings deduced from mechanical properties and gel content analysis that in both SEBS/TPU and SEBS-g-MA/TPU systems, there is a considerable formation of crosslinked networks due to EB treatment. However, irradiated SEBS/TPU blends exhibited the highest gel content in them, preferably as a result of crosslinked individual clusters. The immense increase in the complex viscosity in this blend system with EB exposure can be correlated to this fact. The value of viscosity at lower frequencies for blends with high 50 and 100 kGy doses of radiation is almost 18 times or more than the unirradiated blends. At higher frequency region, the polymer chains undergo breakdown, and hence the value decreases. It is clear from Table 4 that maleated SEBS/TPU blends upon irradiation show a three to four times

TABLE 4 Melt-rheological parameters from parallel plate rheometer

Sample name	Complex viscosity at 0.05 rad/s (pa.s)	Slope (n)	Consistency index (k)
$S_{60}T_{40}$_0 kGy	131,917	−0.88	9228
$S_{60}T_{40}$_10 kGy	68,075	−0.59	11,565
$S_{60}T_{40}$_25 kGy	181,776	−0.85	14,180
$S_{60}T_{40}$_50 kGy	2,617,020	−0.90	174,813
$S_{60}T_{40}$_100 kGy	2,819,990	−0.92	180,601
$M_{60}T_{40}$_0 kGy	158,519	−0.68	20,186
$M_{60}T_{40}$_10 kGy	134,251	−0.68	17,253
$M_{60}T_{40}$_25 kGy	184,635	−0.73	20,936
$M_{60}T_{40}$_50 kGy	381,919	−0.78	36,142
$M_{60}T_{40}$_100 kGy	605,358	−0.81	53,828

increase in complex viscosity. Accordingly, the consistency index (k) of both systems followed the same pattern of viscosity. Hence it can be concluded from here that the rheological behavior of both SEBS/TPU and SEBS-g-MA/TPU when exposed to EB, is similar.

3.6 | Differential scanning calorimetry

DSC thermograms of the irradiated blends are shown in Figure 11 given below. Endothermic heat flow versus temperature data from the second heating cycle is considered in order to dodge the thermal history of the specimens.[32–35] Hence, the second heating curves of different irradiated blends are given in the figure below.

Glass transition temperatures (T_g) of the samples are marked in the figure, and the values are reported in Table 5 also. The first T_g of the blends is detected at the range of −60–−57°C. The T_g of the polyurethane phase being adjacent to that of the ethylene-butylene domain is seen to be overlapping with the transition noted above.[29] From the observations, it can be found that in SEBS/TPU irradiated blend system, the T_g tends to decrease at higher radiation doses. Glass transition of ethylene-butylene domain decreases from −62.3 to −67.7°C for blends irradiated with 10 kGy and 50 kGy, respectively as distinguishable from thermogram 11(a). The shift in glass transition temperature to the negative region indicates the pronounced effect of chain scission in the blends with EB exposure.

Nevertheless, in SEBS-g-MA/TPU blends an opposite variation in glass transition was detected, that is, the glass transition was shifted slightly to the positive side with respect to the radiation dose. This behavior is indicative of crosslinking between the polymer chains. It is again clear from here that in SEBS-g-MA/TPU blends, crosslinking dominates over chain scission. Also, the extent of compatibility between the two phases in this system plays a vital role in the crosslinking reactions. There are chances of an increase in the miscibility of the components as a consequence of radiation exposure.[5] However, in SEBS/TPU blends, EB radiation is found not to affect the interfacial interactions between the components.

The melting endotherm of the blends has also been analyzed from the thermograms. When considering SEBS/TPU blends, there are two melting temperatures observed during the heating scan. The first T_m is detected

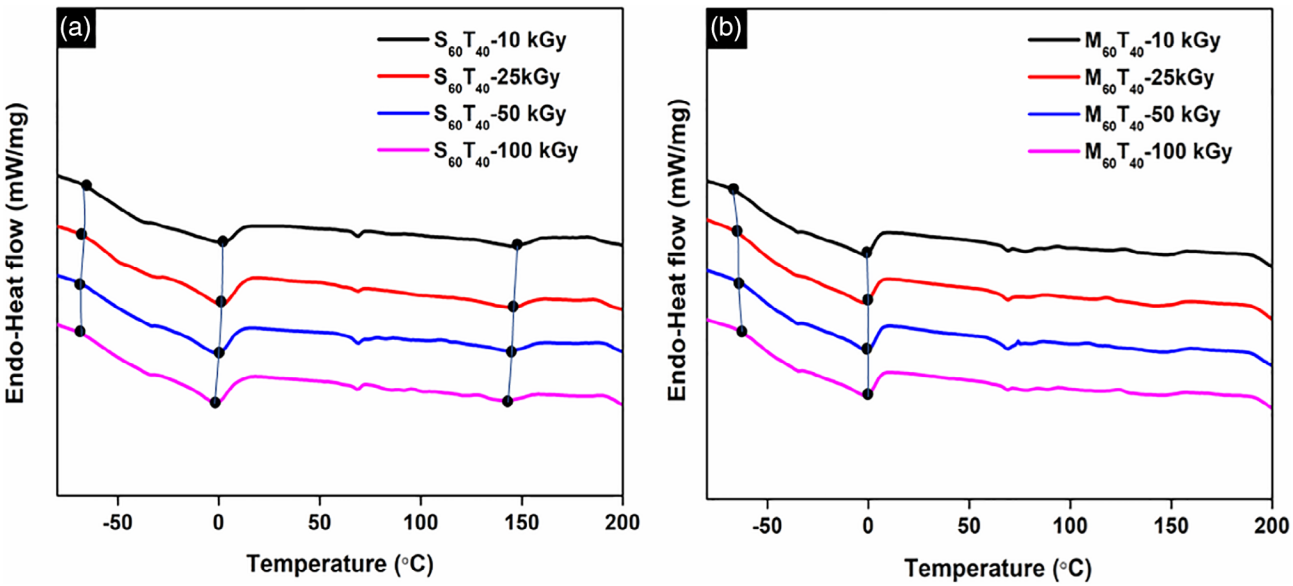

FIGURE 11 Differential scanning calorimetry (DSC) thermograms of (a) $S_{60}T_{40}$ blends (b) $M_{60}T_{40}$ blends after radiation treatment [Color figure can be viewed at wileyonlinelibrary.com]

TABLE 5 Glass transitions, melting endotherms, and heat of fusion of the blends after radiation

Sample	T_{g1} (°C)	T_{m1} (°C)	T_{m2} (°C)	ΔH_f (T_{m1}) (J/g)	ΔH_f (T_{m2}) (J/g)
$S_{60}T_{40}$–10 kGy	−62.3	2.2	146.6	7.5	2.3
$S_{60}T_{40}$–25 kGy	−61.3	1.1	145.1	9.3	2.3
$S_{60}T_{40}$–50 kGy	−67.7	−0.7	143.2	8.9	2.4
$S_{60}T_{40}$–100 kGy	−64.5	−1.7	142.2	8.7	1.8
$M_{60}T_{40}$–10 kGy	−60.0	−1.7	—	6.9	—
$M_{60}T_{40}$–25 kGy	−61.0	1.7	—	7.9	—
$M_{60}T_{40}$–50 kGy	−59.0	−0.7	—	7.7	—
$M_{60}T_{40}$–100 kGy	−58.6	−0.7	—	6.9	—

at around 2.2°C for 10 kGy dose radiated blend, which can be associated with the melting of soft polyol segments in TPU. It shifts to lower temperatures with an increase in radiation dose. It can be attributed to the incompatibility of the components, and the EB exposure did not result in interfacial crosslinking of the polymers. The second melting transition that occurs at 146.6°C due to the hard isocyanate segments is also found to decrease with radiation exposure. On the other hand, in SEBS-g-MA/TPU blends, the changes in melting endotherm are remarkably different from the former system. Most importantly, there is no sharp second melting transition in the blends since the isocyanate groups in TPU react with the maleic anhydride groups in SEBS-g-MA, resulting in the formation of an imide group.[29]

The reactive blends, however, shows the first melting endotherm, and is slightly affected by the EB exposure. There is a minor transition of T_{m1} towards higher temperatures. This is indicative of the formation of crosslinked networks in the system.[8]

The heat of fusion (ΔH_f) of the blends is also reported in Table 5. A high value of ΔH_f is indicative of the crystallinity in the samples. The blend systems used in the study is of rubbery nature and thereby mostly amorphous. However, the semicrystalline nature of TPU contributes to the overall crystallinity of the samples. As concluded from previous observations, the destruction of crystallites by EB radiation can be one of the reasons for the deterioration of mechanical properties. In radiation-resistant TPU, the chances of chain crosslinking or degradation are minimal. The heat of fusion measured from DSC tends to increase slightly first due to some structural reordering. But at higher radiation doses, ΔH_f decreases, indicating destruction of the crystalline phase. Radiation effects on crystallinity are further evaluated through X-Ray Diffraction in the current paper.

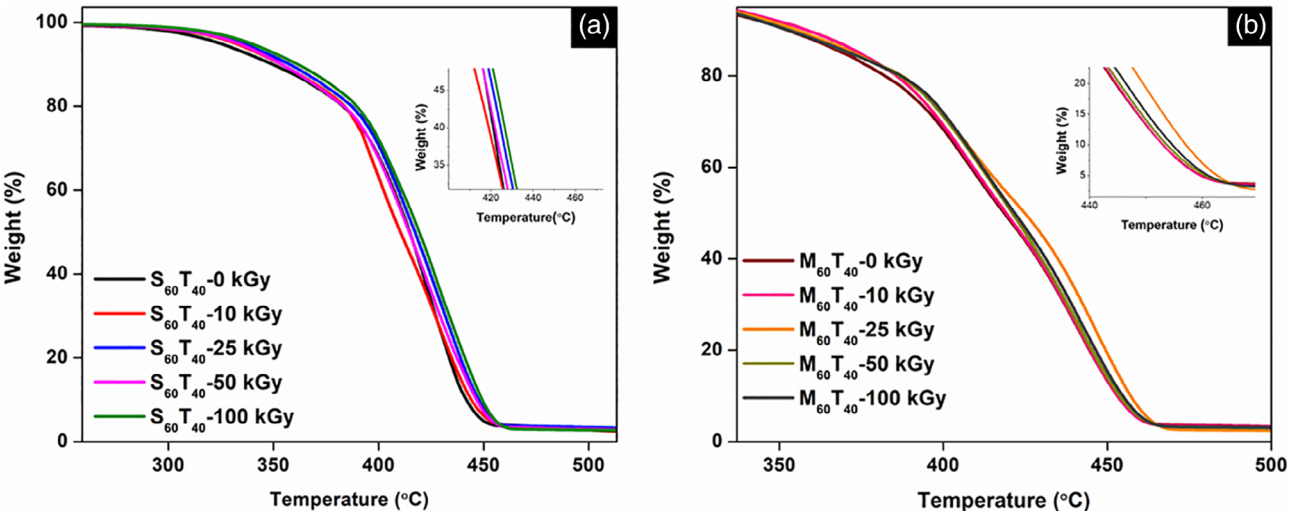

FIGURE 12 Thermogravimetric analysis (TGA) thermograms of (a) $S_{60}T_{40}$ blends (b) $M_{60}T_{40}$ blends before and after radiation treatment [Color figure can be viewed at wileyonlinelibrary.com]

TABLE 6 Thermal decomposition data of irradiated $S_{60}T_{40}$ and $M_{60}T_{40}$ blends

Sample	T_{95} (°C)	T_{50} (°C)	T_{max} (°C)
$S_{60}T_{40}$–0 kGy	324	414	458
$S_{60}T_{40}$–10 kGy	331	422	461
$S_{60}T_{40}$–25 kGy	335	417	461
$S_{60}T_{40}$–50 kGy	333	414	463
$S_{60}T_{40}$–100 kGy	339	419	465
$M_{60}T_{40}$–0 kGy	328	418	467
$M_{60}T_{40}$–10 kGy	333	419	467
$M_{60}T_{40}$–25 kGy	332	424	470
$M_{60}T_{40}$–50 kGy	330	420	471
$M_{60}T_{40}$–100 kGy	329	421	473

3.7 | Thermogravimetric analysis

The assessment of the durability of polymers at a higher temperature is imperative when it comes to their end-use applications. TGA is a key technique in determining the thermal stability and heat resistivity of polymer blends when subjected to a gradual increase in temperature. The inert Nitrogen atmosphere used for the experiment is suitable for thermal analysis based on the total mass loss in the samples.[55] EB irradiation in polymers tends to increase their thermal stability.[27] TGA thermograms depicting temperature versus weight loss of SEBS/TPU and SEBS-g-MA/TPU blends before and after irradiation are shown in Figure 12a, b. Although the temperature range of the test was from 30°C to 700°C, in order to better comprehend the fluctuations, the temperature region of 200–500°C is depicted in the figure. Further, an enlarged view of the thermograms is given alongside the figure. The decomposition data of the samples are tabulated in Table 6. T_{95}, T_{50}, and T_{max} represent the temperature at which 5%, 50%, and maximum weight loss occur, respectively.

The decomposition behavior of SEBS, SEBS-g-MA, and TPU is known from our previous studies. For SEBS and SEBS-g-MA, decomposition starts at around 380°C, and for TPU, it is ~280°C. From Figure 12, it is evident that the major mass loss of the blends befalls between 380 and 470°C. In blend system $S_{60}T_{40}$, the initial decomposition temperature (T_{95}) rises from 324°C to 339°C upon EB irradiation giving a 15°C improvement. T_{95} and T_{max} also tend to improve slightly after exposure to radiation. $M_{60}T_{40}$ system also shows moderate enhancement in the specified temperature values. Upon irradiation, the radicals generated from the labile hydrogens in the polymer recombine engendering crosslinks in the main chain. There are chances of re-association of polymer radicals, also formed due to EB radiation. In either way, C-C bonds formed are highly stable, which imparts improved thermal stability to the polymer chains.[56]

3.8 | X-ray diffraction

XRD of unirradiated and irradiated blends was carried out to understand the structural differences materialized

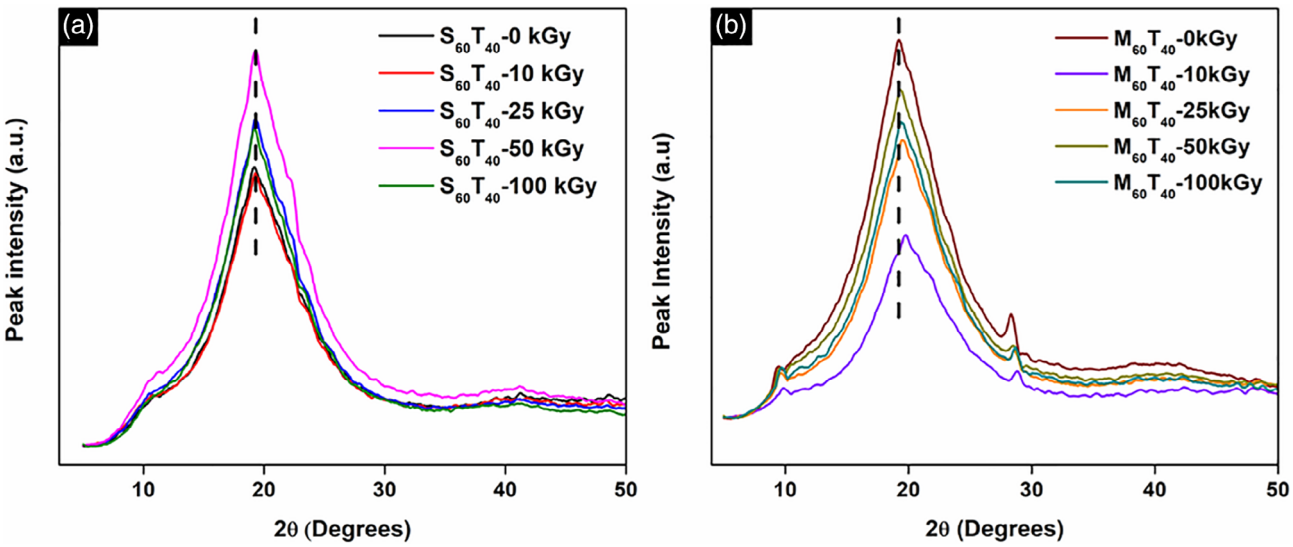

FIGURE 13 XRD patterns of (a) $S_{60}T_{40}$ blends (b) $M_{60}T_{40}$ blends before and after electron beam curing [Color figure can be viewed at wileyonlinelibrary.com]

during the radiation process and to support the observations made earlier. The diffraction spectra of both the systems are depicted in Figure 13a, b.

It is known that the characteristic peak (2θ) of pure SEBS[57] is around 20°, and for pure TPU, this falls around 21°.[58,59] On the other hand, SEBS-g-MA shows an additional minor peak at 28.4°, characteristic of the maleic anhydride group. In both the blend systems, an amorphous halo is observed at an angular range (2θ) of 19.2°. The appearance of halo implies the predominant amorphous state of the polymer blends.[60] From the diffraction angle and wavelength of the X-ray, the interplanar distance was calculated using the Bragg's law and was found to be 0.461 nm. However, the changes in peak intensity upon EB irradiation of the blends are worth noting. For the first set of blends represented in Figure 13a, the peak intensity is found to escalate with radiation dose up to 50 kGy. It indicates certain structural order occurring as a result of radiation.[24] However, at 100 kGy the intensity and diminishes due to associated crosslinking and chain scission.[61] Meanwhile, in SEBS-g-MA/TPU system depicted in Figure 13b, the intensity of the peak decreases suddenly upon EB irradiation, signifying the crosslinking of the polymer chains. Although at higher radiation doses, structural ordering of a certain extent takes place in the blends.

4 | CONCLUSIONS

In this study, the effect of EB treatment in SEBS/TPU and SEBS-g-MA/TPU blends was investigated. The TS along with elongation at break of SEBS/TPU blends deteriorates drastically with EB exposure. The incompatibility between SEBS and TPU and thereby the absence of interfacial crosslinking can be attributed to the observations made. However, SEBS-g-MA/TPU blends showed improvement in TS at first, followed by a minor decrease at a higher dose of radiation. This indicated improvement in the interfacial interaction between SEBS-g-MA and TPU with EB induced crosslinking. The modulus and hardness, however, improved for both the systems suggesting the presence of crosslinks in blend pair. The sol–gel analysis revealed that gel fraction in the SEBS/TPU system is higher suggesting crosslinking in SEBS phase in the presence of TPU. From Charlesby-Pinner the balance between crosslinking and chain scission as a function of radiation dose is determined. The results indicated chain crosslinking in both the blend systems as a result of radiation exposure. The changes in morphology were evaluated from SEM and AFM. The surface roughness was found to increase with radiation dose up to 50 kGy and then decrease at 100 kGy due to higher number of protuberances. From the rheological analysis, the complex viscosity was found to increase profoundly, suggesting the presence of highly crosslinked networks in both the systems. From DSC, the glass and melting transitions were determined along with the heat of fusion. The crystallinity of the samples was affected at higher radiation doses as evidenced from ΔH_f and XRD spectrum. The thermal stability of both blends improved slightly with radiation exposure. Radiation curing was found effective in SEBS-g-MA/TPU blends up to a dose of 25 kGy in terms of mechanical properties. In the SEBS/TPU system, even though crosslinking occurs, the absence of compatibility of the components adversely affected the improvement in performance properties.

ACKNOWLEDGMENTS

The authors would like to thank the Indian Institute of Technology for providing financial assistance to accomplish the work. We are thankful to Dr. Y. K. Bhardwaj, Radiation Technology Development Division, Bhabha Atomic Research Centre, Mumbai, for his assistance in the EB treatment of the samples. We acknowledge the Department of Chemical engineering, Rijksuniversiteit Groningen, the Netherlands, for giving the opportunity to carry out thermal and rheological studies of the samples. We also acknowledge the suggestions and support of Dr. Sanjay Pal, Aswathy T.R, Asit Baran Bhattacharya, Sreethu T.K, and Jeevanandham.

CONFLICT OF INTEREST

The authors have no conflict of interest.

ORCID

M. G. Anagha https://orcid.org/0000-0002-4607-0325
Kinsuk Naskar https://orcid.org/0000-0002-8536-4983

REFERENCES

[1] A. Charlesby, *Atomic Radiation and Polymers*, Pergamon Press Ltd, London **1960**.
[2] H. E. Charles, K. F. James, *Radiation Curing of Polymeric Materials*. ACS Symposium Series, **1990**, p 567.
[3] A. K. Bhowmick, V. Vijayabaskar, *Rubber Chem. Technol.* **2006**, *79*, 402.
[4] K. S. Bandzierz, L. A. E. M. Reuvekamp, G. Przybytniak, W. K. Dierkes, A. Blume, D. M. Bieliński, *Radiat. Phys. Chem.* **2018**, *149*, 14.
[5] V. Mittal, in *Functional Polymer Blends: Synthesis, Properties, and Performance* (Ed: V. Mittal), CRC Press, Boca Raton **2012**.
[6] J. White, S. K. De, K. Naskar, *Rubber Technologist's Handbook*, Vol. 2, Rapra Technology Limited, Shawbury **2009**.
[7] A. K. Bhowmick, H. L. Stephens, *Handbook of elastomers*; Marcel Dekker, Inc, New York **2001**.
[8] T. Chatterjee, S. Wiessner, Y. K. Bhardwaj, K. Naskar, *Mater. Sci. Eng. B Solid-State Mater. Adv. Technol* **2019**, *240*, 75.

[9] R. Giri, K. Naskar, G. B. Nando, *Radiat. Phys. Chem.* **2012**, *81*, 1930.
[10] J. Dutta, T. Chatterjee, G. Dhara, K. Naskar, *RSC Adv.* **2015**, *5*, 41563.
[11] S. Chattopadhyay, T. K. Chaki, A. K. Bhowmick, *J. Appl. Polym. Sci.* **2001**, *79*, 1877.
[12] J. G. M. Van Gisbergen, W. F. L. M. Hoeben, H. E. H. Meijer, *Polym. Eng. Sci.* **1991**, *31*, 1539.
[13] R. Steller, D. Zuchowska, W. Meissner, D. Paukszta, J. Garbarczyk, *Radiat. Phys. Chem.* **2006**, *75*, 259.
[14] L. Yun-yong, Z. Tao, G. Yan, Z. Ai-ming, *Polym. Mater.: Sci. Eng.* **2006**, *5*, 140.
[15] F. Lu, Y. Liu, S. Gao, D. Y. Li, Y. L. Mai, H. H. Shi, W. Hu, *Polym. Bull.* **2020**, *78*, 3293.
[16] G.-M. Kim, G. H. Michler, J. Rösch, R. Mülhaupt, *Acta Polym.* **1998**, *49*, 88.
[17] Y. Li, T. Xie, G. Yang, *J. Appl. Polym. Sci.* **2005**, *95*, 1354.
[18] A. M. Gopalan, K. Naskar, *Polym. Adv. Technol.* **2019**, *30*, 608.
[19] K. Bagdi, K. Molnár, I. Sajó, B. Pukánszky, *Express Polym. Lett.* **2011**, *5*, 417.
[20] J. Dutta, K. Naskar, *RSC Adv.* **2014**, *4*, 60831.
[21] Q. W. Lu, C. W. Macosko, *Polymer (Guildf).* **2004**, *45*, 1981.
[22] E. Adem, E. Angulo-Cervera, A. González-Jiménez, J. L. Valentín, A. Marcos-Fernández, *Radiat. Phys. Chem.* **2015**, *112*, 61.
[23] K. A. Murray, J. E. Kennedy, B. McEvoy, O. Vrain, D. Ryan, R. Cowman, C. L. Higginbotham, *Eur. Polym. J.* **2013**, *49*, 1782.
[24] Q. Tian, E. Takács, I. Krakovský, Z. E. Horváth, L. Rosta, L. Almásy, *Polymers (Basel).* **2015**, *7*, 1755.
[25] M. Walo, G. Przybytniak, K. Łyczko, M. Piatek-Hnat, *Radiat. Phys. Chem.* **2014**, *94*, 18.
[26] J. Dutta, P. Ramachandran, S. M. R. S. Ismail, K. Naskar, *Polym. - Plast. Technol. Eng* **2017**, *56*, 421.
[27] M. M. H. Senna, Y. K. Abdel-Moneam, Y. A. Hussein, A. Alarifi, *J. Appl. Polym. Sci.* **2012**, *125*, 2384.
[28] M. Zenkiewicz, M. Rauchfleisz, J. Czupryńska, J. Polański, T. Karasiewicz, W. Engelgard, *Appl. Surf. Sci.* **2007**, *253*, 8992.
[29] M. G. Anagha, K. Naskar, *J. Appl. Polym. Sci.* **2019**, *48727*, 1.
[30] V. L. Auslender, V. V. Bezuglov, A. A. Bryazgin, V. A. Gorbunov, V. G. Cheskidov, I. V. Gornakov, B. L. Faktorovich, V. E. Nekhaev, V. S. Podobaev, A. D. Panfilov, A. V. Sidorov, V. O. Tkachenko, A. F. Tuvik & L. A. Voronin RuPAC 2006 Contributions to the Proceedings - 20th Russian Conference on Charged Particle Accelerators 2006, p. 126.
[31] S. Anandhan, P. P. De, S. K. De, S. Bandhopadhyay, A. K. Bhowmick, *J. Mater. Sci* **2003**, *8*, 2793.
[32] S. Remanan, M. Bose, A. K. Das, N. C. Das, *J. Appl. Polym. Sci.* **2019**, *136*, 136.
[33] S. M. R. Paran, H. Vahabi, F. Ducos, K. Formela, P. Zarrintaj, A. Laachachi, J. M. Lopez Cuesta, M. R. Saeb, *J. Appl. Polym. Sci.* **2018**, *135*, 135.
[34] S. Saha, A. K. Bhowmick, *Rubber Chem. Technol.* **2018**, *91*, 268.
[35] M. T. Kalichevsky, J. M. Blanshard, *Carbohydr. Polym.* **1992**, *19*, 271.
[36] T. Chatterjee, S. M. R. Syed Ismail, R. Padmanabhan, K. Naskar, *Polym. Adv. Technol.* **2017**, *28*, 686.
[37] P. Svoboda, D. Svobodova, P. Mokrejs, V. Vasek, K. Jantanasakulwong, T. Ougizawa, T. Inoue, *Polymer (Guildf).* **2015**, *81*, 119.
[38] E. Kontou, G. Spathis, M. Niaounakis, V. Kefalas, *Colloid Polym. Sci.* **1990**, *268*, 636.
[39] S. Chattopadhyay, T. K. Chaki, A. K. Bhowmick, *J. Appl. Polym. Sci.* **2001**, *81*, 1936.
[40] R. Gottlieb, T. Schmidt, K. F. Arndt, *Nucl. Instruments Methods Phys. Res. Sect. B Beam Interact. with Mater. Atoms* **2005**, *236*, 371.
[41] Z. Wanxi, H. Tianbai, S. Jiazhen, Q. Baogong, *Int. J. Radiat. Appl. Instrumentation. Part* **1989**, *33*, 581.
[42] T. Zaharescu, R. Setnescu, S. Jipa, T. Setnescu, *J. Appl. Polym. Sci.* **2000**, *77*, 982.
[43] M. R. Vanlandingham, R. F. Eduljee, J. W. Gillespie, *J. Appl. Polym. Sci.* **1999**, *71*, 699.
[44] S. N. Magonov, V. Elings, V. S. Papkov, *Polymer (Guildf).* **1997**, *38*, 297.
[45] T. H. Fang, W. J. Chang, *J. Phys. Chem. Solids* **2003**, *64*, 913.
[46] K. C. Khulbe, C. Y. Feng, T. Matsuura, *Synthetic Polymeric Membranes- Charactreization by Atomic Force Microscopy*, Springer, Berlin Heidelberg **2008**.
[47] A. A. El-Saftawy, A. Elfalaky, M. S. Ragheb, S. G. Zakhary, *Radiat. Phys. Chem.* **2014**, *102*, 96.
[48] L. Yang, J. Chen, Y. Guo, Z. Zhang, *Appl. Surf. Sci.* **2009**, *255*, 4446.
[49] R. Nathawat, A. Kumar & Y. K. Vijay Proc. IEEE Part. Accel. Conf. 2007, 2745.
[50] R. Nathawat, A. Kumar, N. K. Acharya, Y. K. Vijay, *Surf. Coatings Technol.* **2009**, *203*, 2600.
[51] B. S. Shin, D. K. Seo, H. Kim, J. P. Bin; Jeun, P. H. Kang, *J. Ind. Eng. Chem* **2012**, *18*, 526.
[52] H. Liu, T. Xie, Y. Ou, X. Fang, G. Yang, *Polym. J.* **2004**, *36*, 754.
[53] S. Datta, K. Naskar, Y. K. Bhardwaj, S. Sabharwal, *Polym. Bull.* **2011**, *66*, 637.
[54] C. Nakason, S. Saiwaree, S. Tatun, A. Kaesaman, *Polym. Test.* **2006**, *25*, 656.
[55] R. T. Subramaniam, R. S. Rajantharan, *Characterization of Polymer Blends: Miscibility, Morphology, and Interfaces*. Wiley-VCH Verlag GmbH & Co. KGaA, Weinheim **2015**, p. 347.
[56] I. Banik, A. K. Bhowmick, S. V. Raghavan, A. B. Majali, V. K. Tikku, *Polym. Degrad. Stab.* **1999**, *63*, 413.
[57] P. Chen, X. Gao, Y. Wang, T. Xu, Y. Fang, Z. Zhang, *Sol. Energy Mater. Sol. Cells* **2016**, *149*, 60.
[58] C. Fang, R. Yang, Z. Zhang, X. Zhou, W. Lei, Y. Cheng, W. Zhang, D. Wang, *RSC Adv.* **2018**, *8*, 8920.
[59] E. Basturk, S. Madakbas, M. V. Kahraman, *Mater. Res.* **2016**, *19*, 434.
[60] B. Jaleh, P. Parvin, N. Sheikh, F. Ziaie, M. Haghshenas, L. Bozorg, *Radiat. Phys. Chem.* **2007**, *76*, 1715.
[61] S. Raghu, K. Archana, C. Sharanappa, S. Ganesh, H. Devendrappa, *J. Radiat. Res. Appl. Sci.* **2016**, *9*, 117.

How to cite this article: M. G. Anagha, T. Chatterjee, F. Picchioni, K. Naskar, *J. Appl. Polym. Sci.* **2022**, *139*(9), e51721. https://doi.org/10.1002/app.51721